Lab on a Chip

Cite this: *Lab Chip*, 2012, **12**, 2015–2017

www.rsc.org/loc

HIGHLIGHT

Research highlights

Šeila Selimović,[ab] Cole A. DeForest,[c] Mehmet R. Dokmeci[ab] and Ali Khademhosseini*[abde]

DOI: 10.1039/c2lc90045a

Hydrodynamic tweezers

Designing efficient and reliable microfluidic devices can be aided through understanding of the physics governing fluid flows inside them. In particular, microfluidic systems can be developed to exploit physical phenomena that only become important on the microscale. For example, surface tension dominates over the gravitational force inside microchannels, and fluids tend to exhibit laminar rather than turbulent flow.[1] However, certain details of flow behaviors, such as formation of eddy currents around physical obstructions, have not been studied in great detail.

To understand the characteristics of eddy formation in oscillatory flows, Schwartz and colleagues studied these flows inside microfluidic channels. Lieu *et al.*[2] fabricated a wide microscale channel with nine specific geometrical features, using standard photo- and soft lithography techniques. The channel embedded in an elastomer incorporated three free-standing features, with circular, square, and diamond-shaped cross-sections. It also contained three types of protrusions and cavities in the channel walls. These features were semi-circular, square, and triangular. The diameter or side length of each feature was 50 μm or a factor of 2*a*, where *a* was the characteristic length and much larger than the oscillation amplitude. The goal of using these 9 different shapes was to observe potential differences in eddy formation.

To analyze the hydrodynamic properties around these structures, fluorescent density-matched polystyrene beads (1 μm) were suspended in water and used as tracer elements. Upon activation of an oscillatory flow that was generated *via* piezo-based controls, these tracer particles moved with the liquid, rather than sinking to the bottom of the channel. During imaging, a relatively long exposure time was used. This resulted in smeared images of the tracer particles, which allowed the researchers to visualize the stream lines. In addition to these experiments, simulations of the flow were conducted. Based on the Navier–Stokes and continuity equations and assuming small oscillations, these simulations generated stream lines that matched the experimental results. Namely, both experiments and simulations suggested that the streaming flows were weakest in the vicinity of the circular obstructions and strongest near the diamond-shaped posts. Similar observations were made for the protrusions and cavities.

The authors also analyzed the effects of oscillating flows on large polystyrene particles that were suspended in the same solution. In these experiments, the particles were 10 μm in size, which was comparable to the characteristic length *a*. For all nine tested geometries, the large particles first followed the stream lines and then became trapped (Fig. 1). Interestingly, the beads were trapped closer to the free-standing features compared to the protrusions and cavities. This was interpreted as a consequence of the eddies, which were stronger near the free-standing obstruction than near the wall features. For 8 out of 9 geometries, the particle trapping was permanent, akin to trapping *via* optical tweezers. Only in the case of the triangular cavity were the "hydrodynamic tweezers" unstable. Here, the eddies were too weak to permanently trap a bead.

This study is valuable for a variety of microfluidic applications in which particles (such as cells or microbeads) are suspended. For example, these results are informative for the design of complex microfluidic structures, such as particle storage wells or cell traps. Furthermore, the hydrodynamic tweezers introduced here can be useful for single-cell experiments as

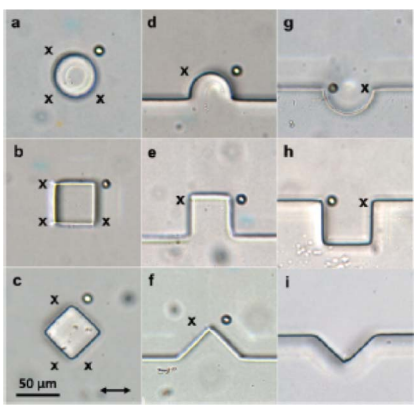

Fig. 1 Polystyrene beads (10 μm), trapped hydrodynamically in eddies near different microscale features: free standing obstructions (a–c), protrusions (d–f) and cavities (g–i). The arrow in (c) indicates the direction of the oscillatory flow. Positions labeled with **x** indicate stable, but empty particle trapping sites. Figure reprinted with permission from Lieu *et al.*[2] Copyright (2012) American Chemical Society.

[a]*Center for Biomedical Engineering, Department of Medicine, Brigham and Women's Hospital, Harvard Medical School, Cambridge, Massachusetts 02139, USA. E-mail: alik@rics.bwh.harvard.edu*
[b]*Harvard-MIT Division of Health Sciences and Technology, Massachusetts Institute of Technology, Cambridge, Massachusetts 02139, USA*
[c]*Division of Chemistry and Chemical Engineering, California Institute of Technology, Pasadena, California 91125, USA*
[d]*Wyss Institute for Biologically Inspired Engineering, Harvard University, Boston, Massachusetts 02115, USA*
[e]*World Premier International – Advanced Institute for Materials Research (WPI-AIMR), Tohoku University, Sendai 980-8577, Japan*

well as particle sorting and shear stress studies. In the future, it would be interesting to study architectural features that give rise to hydrodynamic trapping in linear flows. In addition, an investigation of tweezers suitable for stable trapping of particle clusters, akin to holographic optical tweezers would represent a great advance in the field.

Combinatorial concentration gradients for drug screening

The drug discovery process represents an important potential application for microfluidic technologies. Since drug-based studies focus on the effects of various combinations of different drugs as well as different drug concentrations on cellular behavior, a high-throughput experimental approach is advantageous. Microfluidics offer the potential for high-throughput testing, in addition to requiring only minute volumes of reagents.[3] Generating many different combinations of two or more drugs has also been achieved in microscale devices. However, developing a simple, programmable microfluidic device capable of both generating a variety of drug mixtures and concentrations, and subsequently applying them to an on-chip cell culture has so far proven challenging.

Recently, Rege, Jayaraman and colleagues have introduced a programmable microfluidic device that offers combinatorial drug screening on an embedded cell array. Fabricated from poly(dimethylsiloxane) (PDMS) *via* standard soft lithography techniques, the device developed by Kim *et al.*[4] included a fluidic layer bonded to a glass slide and a control layer above it. The fluidic layer contained 64 microwells connected to a concentration gradient generator (CGG) *via* fluidic channels. The control layer contained 8 sets of microvalves, designed to connect or isolate individual rows of microwells from the fluidic channels.

The operation of the device is outlined in Fig. 2. First, a solution representing a cell suspension was introduced into the device (a) and was stored in the microwells (b). Then, the CGG was activated to form a gradient of two miscible aqueous solutions S_1 and S_2, where $S_1 = A_0$ + buffer and $S_2 = A_0 + B$ (c). Here, A_i and B represent two solutions, *e.g.* two drugs. Only one row of microwells

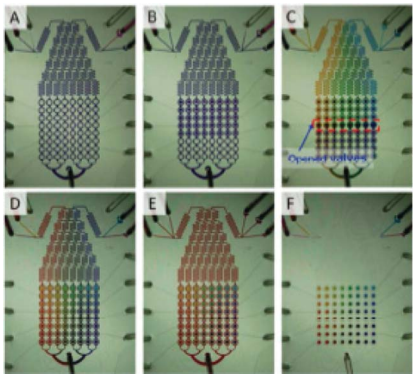

Fig. 2 Operational sequence of the microfluidic device for drug discovery applications: isolation (a) and loading (b) of cell culture wells. Generation of the diffusive concentration gradient (c) and filling of the wells (d). Various combinations of dyes inside the wells before (e) and after (f) washing of the chip. Scale bar: 30 μm. Figure adapted and reprinted with permission from the Royal Society of Chemistry from Kim *et al.*[4]

was connected to the fluidic channels at a time, so that the particular concentration gradient could be used to fill only those wells (d). Next, a new concentration gradient was formed, but this time the relative concentrations of the two solutions were altered. For example, $S_1 = A_1$ + buffer and $S_2 = A_1 + B$ were used. Then, this gradient was connected to another row of wells and the two process steps would be repeated until all microwells were filled with some mixture of the solutions A_i and B (e). Finally, all wells were completely isolated from the fluidic channels (f). During a multi-day experiment, the cell medium inside the microwells was refreshed every 3 h. Here, first all fluidic channels were rinsed with PBS to remove traces of the drug and then the loading process was repeated. It is noteworthy that at this point an entirely new set of drug mixtures could be introduced into the wells or the original drug mixtures could be generated. Thus, both simultaneous as well as sequential testing of drugs and other compounds on cells is enabled.

Another important characteristic of the device was that the activation of valves and the syringe pump driven flows of all solutions were programmed and controlled using a LabView interface. In addition, it was shown that the valves were operating efficiently over the period of several days and therefore no unwanted mixing of the solutions occurred. Thus, a great benefit of this microfluidic device was that no manual handling was necessary. Furthermore, the device was shown to be suitable for cell culture, as cells remained viable for over 5 days inside the microwells.

The utility of this device was exemplified in an experiment on prostate cancer cells (PC3 cell line). The cells were exposed to varying mixtures of the drugs doxorubicin, mitoxantrone and TRAIL, a ligand known for inducing apoptosis in cancer cells. The capability of the device to generate 64 combinations of these molecules within a few minutes enabled better understanding of their effects on the cells. For example, it was shown that the cell viability decreased most when doxorubicin or mitoxantrone were given to the cells 24 h before introducing TRAIL, thus potentially increasing the cell sensitivity to the ligand. The viability decrease was smaller when either of the drugs and TRAIL were administered simultaneously. The lowest loss of viability was observed in cells that had received only one of the drugs or the ligand. Control experiments conducted on a well-plate yielded qualitatively similar results, but generally lower viability values. It was hypothesized that the microfluidic environment (periodic refreshment of medium, potential adsorption of the drugs onto the PDMS walls, comparatively high cell concentrations) was more conducive to cell survival than the well plate.

The many benefits of the microfluidic approach for drug screening presented here are clear. They include the computer control of the fluidic processes, little exposure of cells to shear stresses, repeated replenishment of medium and removal of metabolic products of the cells *etc.* However, the chief improvement compared to the standard approach – the well-plate cell culture – is the automated preparation of 64 distinct drug mixtures. The presented work shows the proof of concept, but it would be a great advance to modify this device into a true high-throughput platform. Such a platform should be capable of generating hundreds, if not thousands of experimental conditions within a short amount of time, and include an automated imaging and analysis system.

Culturing endothelial cells on micropillars

Though it is well established that the extracellular matrix (ECM) affects native cell function *via* the presentation of a myriad of biochemical ligands that interact with cell surface receptors, an emerging appreciation for the influence of ECM compliance (*e.g.*, stiffness) and topographical roughness on cell fate has been gained over the past decade.[5] As the specific effects of these biophysical cues are difficult to assay *in vivo*, researchers have turned towards synthetic *in vitro* culture platforms that enable the induced cell responses from individual network properties to be isolated and studied in a fully user-defined environment.

Combinatorial-based approaches have proven invaluable in extending these fundamental studies to include the synergistic effects of multiple cues on cell fate. Here, advances in micro- and nanofabrication techniques, coupled with the relatively small size scale of an individual cell (*e.g.*, $\sim$10 μm diameter for mammalian cells), enables thousands of physiologically-relevant experimental conditions to be replicated many times over on a single 1 cm^2 chip substrate.

Recently, Dickinson *et al.* have introduced an approach to create combinatorial microarrays to determine the influence of topographical features and network elasticity on endothelial cellular functions.[6] As these cells are responsible for the formation of functional blood vessels *via* angiogenesis that are present in many organs throughout the body, understanding endothelial cell response to environmental cues has significant implications in the fields of regenerative medicine and tissue engineering. In this work, the authors exploit i-line lithography followed by a timed reactive ion etch to fabricate surfaces containing 150 distinct micropillar arrays with features ranging from 1 to 5.6 μm in diameter, heights of 1, 3, 6, or 8 μm, and interpillar spacing ranging between 0.6 to 15 μm. These materials were created from either a stiff SiO_2 or a softer PDMS to examine the effects of material rigidity on cell function. Each type of material was covalently modified with fibronectin, an ECM protein known to promote cell adhesion, to enable cell interaction with the material surface. In addition to full surface biofunctionalization, patterned substrates were generated using a fibronectin-coated PDMS stamp that gave rise to 40 μm wide bioactive stripes across the pillar surface.

For a given topographic feature diameter and spacing, epithelial cells exhibited decreased spreading and viability with increased feature height, and ultimately preferred heights of $<$3 micron. The density of adhesive cellular protrusions differed based on topographical diameter and spacing, where "flat" patterns of large diameter micropillars with small spacing induced few process extensions. Conversely, more pronounced protrusions were observed with smaller pillar diameters and increased spacing. This indicated that there is a window of optimal micropillar array dimensionality that facilitates endothelial cell extension. Moreover, cells cultured on the soft PDMS micropillared substrates achieved a more elongated morphology than those cultured on the stiff SiO_2 micropillars or the flat substrates of either composition, further suggesting the importance of network stiffness on cell elongation and aligned adhesion.

The power of the approach taken by Dickinson *et al.* largely stems from its versatility. Different cell types can be readily cultured on a vast number of topographical microenvironments of varying mechanical properties in order to screen which biophysical parameters give rise to optimal cell function rapidly. This approach will undoubtedly prove fruitful in better understanding basic biological functions and directing cell fate.

References

1 H. A. Stone, A. D. Stroock and A. Ajdari, Engineering flows in small devices. Microfluidic: toward a Lab-on-a-Chip, *Annu. Rev. Fluid Mech.*, 2004, **36**, 381–411; T. M. Squires and S. R. Quake, Microfluidics: Fluid physics at the nanoliter scale, *Rev. Mod. Phys.*, 2005, **77**, 977–1026.
2 V. H. Lieu, T. A. House and D. T. Schwartz, Hydrodynamic Tweezers: Impact of Design Geometry on Flow and Microparticle Trapping, *Anal. Chem.*, 2012, **84**, 1963–1968.
3 P. S. Dittrich and A. Manz, Lab-on-a-chip: microfluidics in drug discovery, *Nat. Rev. Drug Discovery*, 2006, **5**, 210–218; D. Lombardi and P. S. Dittrich, Advances in microfluidics for drug discovery, *Expert Opin. Drug Discovery*, 2010, **5**(11), 1081–1094.
4 J. Kim, *et al.*, A programmable microfluidic cell array for combinatorial drug screening, *Lab Chip*, 2012, **12**, 1813–1822, DOI: 10.1039/c2lc21202a.
5 A. J. Engler, *et al.*, Matrix Elasticity Directs Stem Cell Lineage Specification, *Cell*, 2006, **126**, 677–689.
6 L. E. Dickinson, *et al.*, Endothelial cell responses to micropillar substrates of varying dimensions and stiffness, *J. Biomed. Mater. Res., Part A*, 2012, **100A**, 1457–1466, DOI: 10.1002/jbm.a.34059.